Phase behavior of physically cross-linked asymmetric random heteropolymers

Simcha Srebnik
Department of Chemical Engineering, Technion-Israel Institute of Technology, Haifa, Israel 32000
(Received 14 April 2005; published 2 November 2005)

We study the phase behavior of physically cross-linked asymmetric copolymer networks where the composition of the minor component is small (<10%). The effects of the degree of cross-linking and monomer-monomer interactions on the microstructure of the network are considered. Two cases of cross-links are considered: (1) cross-linking of the majority component only, i.e., inhomogeneous cross-linking, and (2) cross-linking between all types of monomers with equal probability. It is found that for a given set of parameters, both the degree of physical cross-linking and competing (segregating) interactions between the monomers can each be used to induce microphase segregation, or the aggregation of the minor component into ordered microdomains. The type of cross-linking is found to affect the final morphology of the gel while interactions enhance the degree of segregation.

DOI: 10.1103/PhysRevE.72.051802 PACS number(s): 82.35.Jk, 81.05.Lg

I. INTRODUCTION

Tailoring the structure and properties of materials on the molecular level in order to control the structure and functionality of materials is leading to important advances in fields such as chromatography, catalysis, and drug release. It has become evident that multicomponent polymeric materials provide a relatively inexpensive and versatile approach for many applications. In particular, the design of "smart" polymers that undergo spontaneous phase transitions in response to environmental changes, or that are capable of specific recognition on the molecular level are attracting increasing attention. As a recent example, a rich phase behavior has been predicted for triblock polyampholytes that display ordered micellar structures or network structure, depending on *p*H [1]. Such a reversible conformational transition is one of many examples of functional polymers, that, in this case, is controlled through differing degrees of association of monomers along the polyampholyte chains.

Another type of smart polymer gels are formed via a recently developed molecular imprinting approach that involves phase inversion of a polymer solution in presence of an imprinting agent whose subsequent extraction results in a coagulated imprinted gel that relies on physical cross-linking to resist deformation under operating conditions [2,3]. As with conventional imprinting approaches [4,5], relatively low imprinting efficiencies (i.e., low capacity of molecule-specific recognition cavities) are achieved with the phase-inversion technique. In this application, too, functional polymer blends have been suggested in order to improve the stability of such physically cross-linked gels [6,7].

Physical constraints, such as entanglements, and loops, have long been considered as significant contributors to gelation of polymers [8–10]. Deliberate physical constraints can also be introduced in the form of weakly associating monomers in the chain, leading to annealed cross-links. The addition of attractive "stickers" in various chain architectures has been shown to produce a rich phase behavior. End-associating polymers have been considered rather extensively both theoretically [11–13] and by means of computer simulations [14,15]. Polymers having a number of stickers along the chain backbone have been studied by Monte Carlo simulations [16,17] and a theoretical model has been suggested for their dynamic behavior [18].

In the sticker models, the associating monomers present a small fraction of the total size of the polymer, such that only very low degrees of cross-linking are considered. Recently, Gutman and Shakhnovich [19] considered the problem of a physically cross-linked random heteropolymer. The model is general in that all monomers may associate with different cross-linking potentials that are dependent on the type of associating monomers. In this work, we build on their model, but concentrate on physical cross-linking of asymmetric random heteropolymer gels where the minor constituent presents up to 10% composition. We analyze conditions that lead to microphase segregation (aggregation) of the minor constituent.

Figure 1 illustrates our model of a cross-linked random heteropolymer. At high temperatures, it can be envisioned that the system is well mixed with small fluctuations in the average local densities of the different monomers, as depicted in Fig. 1. As the temperature is reduced, however, and the critical point is approached, the homogeneous mixed phase begins to show large fluctuations in the local monomer concentrations, and beyond the critical temperature two distinct microphases of the different monomers exist. The threshold at which the system breaks up spontaneously into domains rich in one type of monomer is known as the spinodal while the process of separation of the monomers into two phase-segregated domains is the spinodal decomposition.

The domain size at the spinodal during the decomposition process can be obtained from light scattering experiments, where the scattering intensity measures segregation that physically reflects the correlation between concentrations of the different monomer types at two points:

$$S_{ij}(r_1 - r_2) = \langle \phi_i(r_1)\phi_j(r_2)\rangle - \langle \phi_i(r_1)\rangle\langle \phi_j(r_2)\rangle, \qquad (1)$$

where S is the correlation function, also called the structure factor; r is the three-dimensional spatial position; ϕ_i and ϕ_j are the volume fractions of the two different monomers. The

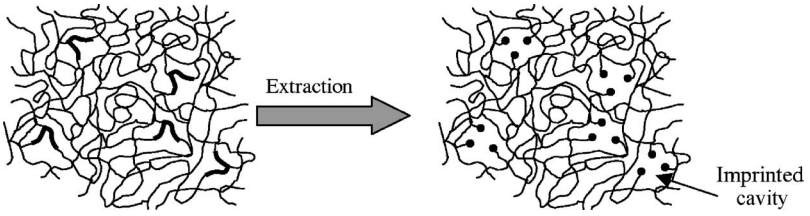

FIG. 1. Two-dimensional schematic depiction of molecular imprinting using a random copolymer with a small fraction of units representing the imprinting molecules (bold lines) and remaining units forming a physically cross-linked and entangled polymer matrix. Solidification of the polymer solution around the imprint molecules occurs quickly using, e.g., the phase inversion technique. Chemical extraction of the minority groups leaves behind cavities complementary to the shape, size, and functionality of the imprinting monomers. Specific functionality of the minority monomers may lead to local distribution of the functional groups within the formed cavities.

spinodal is then the point at which the scattering intensity diverges.

Such a model of physically cross-linked asymmetric random copolymers has implications towards another class of smart polymers which consists of formation of a permanent porous structure that is capable of molecular recognition. In our model, the minor constituent represents, for example, a covalently-bonded imprinting agent. For such applications, conditions that disfavor aggregation of the minor constituent into microphase-segregated domains are beneficial.

The organization of the manuscript is as follows: In Sec. II we develop the model of a physically cross-linked asymmetric polymer using the path-integral formulation and obtain an expression for the free energy. In Sec. III we analyze conditions that lead to transition form a disordered phase to a microphase segregated phase. In Sec. IV we present some concluding remarks and briefly discuss the implications of our model towards molecular imprinting.

II. MODEL DEVELOPMENT

In this section we develop a mean-field model for cross-linked copolymer networks composed mostly of one type of monomer, say A, covalently bonded to the functional minor constituent, B. We model a cross-linked random copolymer chain made up of a large number of monomers, N, of which a fraction f are backbone monomers of type $A(f\sim 1)$ and the remainder constitutes the "imprinting" B monomers. The distribution of A and B segments is taken to be Gaussian with a mean $\bar{\theta}=(2f-1)$ and variance $\sigma^2=4f(1-f)$. For bulk properties, end-effects can be neglected and such a representation of cross-linked polymer networks is appropriate [20,21]. The partition function, Z, of a copolymer chain subject to the constraint of forming N_{cl} cross-links (formed from $2N_{\mathrm{cl}}$ monomers) can be written using Feynman's path integral formulation as [22]

$$Z=\iint Dr(s)\exp\left(-\frac{1}{2a^2}\int_0^N ds\left(\frac{\partial r}{\partial s}\right)^2 - \frac{1}{2}\sum_{I,J}\int_0^N ds\int_0^N ds'(V_{IJ}[r(s)-r(s')]\delta_{IJ})\right) \times \prod_{I,J}\prod_{i=1}^{N_{IJ}}\int_0^N ds\int_0^N ds'\,\delta_{IJ}\delta[r_{Ii}(s)-r_{Ji}(s')], \qquad (2)$$

where a is the monomer size, assumed to be equal for both A and B. $r(s)$ is the spatial location of the monomer at position s along the backbone of the chain. The summation and product subscripts I and J are over the types of monomers and for our system are either A- or B-type monomers, contributing three terms for such binary systems (i.e., $I=J=A$; $I=J=B$; and $I=A$, $J=B$). V_{IJ} is the monomer-monomer interaction potential between I-type monomer at position $r(s)$ and J-type monomer at position $r(s')$. The Kronecker delta, δ_{IJ}, is included so that only appropriate monomer pairs contribute to each type of interaction potential and cross-linking pairs. The product term enforces N_{IJ} cross-links between the different types of monomers, such that $N_{\mathrm{cl}}=\frac{1}{2}\Sigma_{I,J}N_{IJ}$. In Eq. (2), the cross-link labeled by the index i connects the I-type monomer at position $r(s)$ with J-type monomer at position $r(s')$, such that only those configurations that satisfy the constraints $r_{Ii}(s)=r_{Ji}(s')$ (with $i=1,\ldots,N_{IJ}$, for I and $J=A$ or B) are retained in the ensemble.

We assume a Poisson distribution of the cross-links, P_{cl}, where the average number of cross-linked monomers is determined by the fugacity of the different monomers, μ_{IJ} [20],

$$P_{\mathrm{cl}}=\left(\frac{e^{\beta\mu_{AA}N_{AA}}}{2!N_{AA}!}\right)\left(\frac{e^{\beta\mu_{AB}N_{AB}}}{N_{AB}!}\right)\left(\frac{e^{\beta\mu_{BB}N_{BB}}}{2!N_{BB}!}\right), \qquad (3)$$

where $\beta=1/k_BT$, k_B is the Boltzmann constant, and T is the temperature. The factorials $N_{IJ}!$ and $2!$ account for the indistinguishable contacts and monomers, respectively.

The Kronecker deltas in Eq. (2) can be written in terms of an Ising-type variable [23], $\theta(s)$, which labels the type of segments encountered at position s, e.g., $\theta(s)=1$ for A-type monomers, and -1 for B. It is also convenient to introduce the following definitions of effective monomer-monomer potentials:

$$V_0=\tfrac{1}{4}(V_{AA}+2V_{AB}+V_{BB}),$$

$$V_D=\tfrac{1}{4}(V_{AA}-V_{BB}),$$

$$V_F=\tfrac{1}{4}(V_{AA}-2V_{AB}+V_{BB})=-\tfrac{1}{2}\chi. \qquad (4)$$

The last definition in Eq. (4) is related to the Flory chi parameter, χ, which is a measure of the difference in the magnitude of interactions between the different monomers. Copolymer systems described by positive values of χ tend to microphase segregation [24].

We assume that the cross-links are reversible once formed and may anneal in response to external changes. Thus, the summation over the distributions of cross-links appearing in Eq. (3) can be readily carried out using the expansion, $e^x = \Sigma_k x^k/k!$,

$$\langle Z\rangle = \iint Dr(s)\exp\left(-\frac{1}{2a^2}\int_0^N ds\left(\frac{\partial r}{\partial s}\right)^2 - \frac{1}{2}\int_0^N ds\int_0^N ds' V_0[r(s)-r(s')]\right) \times\exp\left(-\frac{1}{2}\int_0^N ds\int_0^N ds'(V_D[r(s)-r(s')]\theta(s) + V_F[r(s)-r(s')]\theta(s)\theta(s'))\right) \times\exp\left(\frac{1}{2}\int_0^N ds\int_0^N ds'(\mu_0 + 2\mu_D\theta(s) + \mu_F\theta(s)\theta(s'))\delta(r(s)-r(s'))\right), \quad (5)$$

where the μ's have analogous definitions as the interactions in Eq. (4), but for the respective fugacities, i.e.,

$$\mu_0 = \tfrac{1}{4}(e^{\beta\mu_{AA}} + 2e^{\beta\mu_{AB}} + e^{\beta\mu_{BB}}),$$

$$\mu_D = \tfrac{1}{4}(e^{\beta\mu_{AA}} - e^{\beta\mu_{BB}}),$$

$$\mu_F = \tfrac{1}{4}(e^{\beta\mu_{AA}} - 2e^{\beta\mu_{AB}} + e^{\beta\mu_{BB}}). \quad (6)$$

Thus, the physical constraints due to the cross-links are replaced by an effective attractive interaction with strength proportional to μ. To proceed with the solution of Eq. (5), we introduce the following order parameters:

$$\rho(r) = \int_0^N ds\,\delta(r(s)-r) \quad (7)$$

and

$$m(r) = \int_0^N ds\,\delta\theta(s)\,\delta(r(s)-r), \quad (8)$$

where $\delta\theta(s) = \theta(s) - \bar{\theta}$ measures the fluctuations in the value of the Ising variable θ from the mean value $\bar{\theta} = 2f - 1$. $\rho(r)$ is the density order parameter. The microphase order parameter, $m(r)$, is a measure of the difference between local densities of the different monomers [22,25–27]. In addition, we define the following effective interactions:

$$v_0(r-r') = V_0(r-r') + 2V_D(r-r')\bar{\theta} + V_F(r-r')\bar{\theta}^2 - (\mu_0 + 2\mu_D\bar{\theta} + \mu_F\bar{\theta}^2)\delta(r-r'),$$

$$v_D(r-r') = V_D(r-r') + V_F(r-r')\bar{\theta} - (\mu_D + \mu_F\bar{\theta})\delta(r-r'),$$

$$v_F(r-r') = V_F(r-r') - \mu_F\delta(r-r'). \quad (9)$$

The following expression for the partition function is obtained after rewriting Eq. (5) in terms of the order parameter fields and the effective interactions, and averaging over the distributions of cross-links,

$$\langle Z\rangle = \iint Dr(s)\iint D\rho(r)\iint Dm(r) \times\exp\left(-\frac{1}{2a^2}\int_0^N ds\left(\frac{\partial r}{\partial s}\right)^2\right) \times\exp\left(-\frac{1}{2}\int dr\int dr'(\rho(r)v_0(r-r')\rho(r') + 2\rho(r)v_D(r-r')m(r') + m(r)v_F(r-r')m(r'))\right) \times\delta\left(\rho(r) - \int_0^N ds\,\delta(r(s)-r)\right) \times\delta\left(m(r) - \int_0^N ds\,\delta\theta(s)\,\delta(r(s)-r)\right). \quad (10)$$

Next, we must average over the monomer sequence distribution which is fixed after preparation. Averages over quenched distributions can be carried out using the replica trick, first introduced in the context of macromolecular networks by Deam and Edwards [20]. In this approach, the system is replicated m times and the quenched randomness is replaced by inter-replica interactions so that quenched averages are calculated over $m+1$ copies of the free energy rather than over the logarithm of the free energy. To obtain the free energy expression, we proceed as in Refs. [26,28] and rewrite the Hamiltonian in terms of effective energy and entropy of the system,

$$\langle Z^m\rangle = \prod_{\alpha=1}^m \iint D\rho^\alpha(\mathbf{r})\iint m^\alpha(\mathbf{r}) \times\exp\left(-\sum_\alpha(\beta E[\rho^\alpha,m^\alpha] - S[\rho^\alpha,m^\alpha])\right), \quad (11)$$

where

$$E[\rho^\alpha,m^\alpha] = \frac{1}{2}\int dr\int dr'(\rho^\alpha(r)v_0(r-r')\rho^\alpha(r') + \rho^\alpha(r)v_D(r-r')m^\alpha(r') + m^\alpha(r)v_F(r-r')m^\alpha(r')) \quad (12)$$

and

$$S[\rho^\alpha,m^\alpha] = \ln\left\{\prod_{\alpha=1}^m\iint Dr^\alpha(s) \times\exp\left(-\frac{1}{2a^2}\sum_\alpha\int_0^N ds\left(\frac{\partial r^\alpha}{\partial s}\right)^2\right) \times\iint D\varphi_\rho^\alpha(r)\exp\left(i\sum_\alpha\int dr\,\varphi_\rho^\alpha(r)\cdot\left(\rho^\alpha(r)\right.\right.\right.$$

$$- \int_0^N ds\,\delta[r^\alpha(s) - r^\alpha]\Big)\Big)$$
$$\times \iint D\varphi_m^\alpha(r)\exp\Big(i\sum_\alpha \int dr\,\varphi_m^\alpha(r)\cdot\Big(m^\alpha(r)$$
$$- \int_0^N ds\,\delta\theta(s)\,\delta[r^\alpha(s) - r^\alpha]\Big)\Big)\Big\}, \quad (13)$$

where we have introduced the delta functions over the order parameter fields appearing in Eqs. (7) and (8) as path integrals. The effective entropy defines the conformation space of the network under the constraints of the order parameter fields.

The effective entropy can be calculated by introducing external fields conjugate to the density and microphase order parameter fields [26]

$$Z^m[\varphi_\rho^\alpha,\varphi_m^\alpha] = \prod_{a,\alpha}\iint D\rho^\alpha(r)\iint Dm^\alpha(r)$$
$$\times\exp\Big(-\sum_\alpha \int dr(\varphi_\rho^\alpha(r)\rho^\alpha(r) + \varphi^\alpha(r)m^\alpha(r))$$
$$+ S[\rho^\alpha,m^\alpha]\Big). \quad (14)$$

We consider a dense network such that the order parameter fields have small fluctuations. Therefore, a saddle-point approximation that minimizes the integrand in Eq. (14) can be used so that the order parameters are determined by

$$\rho^\alpha = -\,\delta \ln Z^p/\delta\varphi_\rho^\alpha,$$
$$m^\alpha = -\,\delta \ln Z^p/\delta\varphi_m^\alpha. \quad (15)$$

In order to calculate $(\ln Z^p)$, the average over the sequence fluctuations is carried out, resulting in

$$Z^m = \prod_\alpha \iint Dr^\alpha(s)\exp\Big\{-\frac{1}{2a^2}\sum_\alpha\int_0^N ds\Big(\frac{\partial r^\alpha}{\partial s}\Big)^2$$
$$-\sum_\alpha\int_0^N ds\,\varphi_\rho^\alpha[r^\alpha(s)] + \frac{\sigma^2}{2}\sum_\alpha\int_0^N ds\Big(\sum_\alpha \varphi_m^\alpha[r^\alpha(s)]\Big)^2\Big\}. \quad (16)$$

The steps taken for the calculation of the entropy appearing in Eq. (14) are outlined in the Appendix. The ground state free energy is obtained by combining the expression for the entropy with that of the energy in Eq. (12),

$$F[\rho^\alpha,m^\alpha] = \tfrac{1}{2}\sum_\alpha\sum_k(\rho^\alpha(k)v_0(k)\rho^\alpha(-k)$$
$$+ 2\rho^\alpha(k)v_D(k)m^\alpha(-k) + m^\alpha(k)v_F(k)m^\alpha(-k))$$
$$+ \sum_\alpha \tilde{\varphi}^\alpha(k=0) - \sum_{a,\alpha}\sum_{k\neq 0}\frac{\tilde{\varphi}^\alpha(k)\tilde{\varphi}^\alpha(-k)}{a^2k^2}$$
$$- \frac{\sigma^4}{4}\sum_{\alpha\neq\beta}\sum_{k,k'\neq 0}\frac{\varphi_m^\alpha(k)\varphi_m^\alpha(-k)\varphi_m^\beta(k')\varphi_m^\beta(-k')}{a^2(k^2+k'^2)}$$
$$- \sum_\alpha\sum_k[\varphi_\rho^\alpha(k)\rho^\alpha(-k) + \varphi_m^\alpha(k)m^\alpha(-k)]. \quad (17)$$

The terms appearing in the first line of Eq. (17) are due to short-ranged interactions between the different monomers (the first term is the excluded volume nonspecific interactions that describe the average interactions felt by the monomers, the second term relates the difference in the interaction values, i.e., $v_D \sim V_A - V_B$, while the last term is related to the Flory two-body specific interactions that are responsible for microphase separation), all rescaled by the cross-linking potentials between the different monomers. The last three lines result from the entropy and reflect how the constraints of cross-linking and the disordered sequence distribution influence microphase ordering. The quadratic terms in the auxiliary fields correspond to the decrease in entropy due to phase separation of the different monomers, not accounting for connectivity and cross-linking. The quartic term that couples different replicas accounts for the effect the connectivity constraints between nearest-neighbor monomers on microphase ordering.

III. RESULTS AND DISCUSSION

In this section, we analyze the nature of the disordered phase in order to gain information on the stability limit beyond which the system drives towards order. Conditions favoring phase separation, which may lead to a distribution of *B*-rich regions that are much larger than a single monomer, can be used to form mesoporous structures once the minority constituent is removed. On the other hand, such aggregation should be avoided if these monomers are to act as individual imprinting agents.

A. Disordered phase

In the analysis of the disordered phase, we can neglect the quartic terms in Eq. (17) when calculating the free energy, which determine the physics of ordered phases [26,28]. Since the remaining terms depend on only one replica index in either the sequence or cross-links replica space, we consider the replica symmetric solution. In this case, solution of Eqs. (A7) and (A8) for auxiliary order parameter fields, φ_ρ and φ_m, results in the following expression for the free energy:

$$F[\rho,m] = \frac{1}{2}\sum_k\Big[\Big(v_0(k) + \frac{a^2k^2}{2}\Big)\rho(k)\rho(-k) + 2v_D(k)\rho(k)m$$
$$\times(-k) + \Big(v_F(k) + \frac{1}{\sigma^2}\Big)m(k)m(-k)\Big]. \quad (18)$$

Scattering experiments can provide information on the structure factor of the cross-linked system, which describes the average correlations between the concentrations of the different monomers. If correlations exist, then the intensity shows a peak at a wavelength corresponding to the typical length scale of correlation. The structure factor can be evaluated through transformation of the 2×2 matrix of quadratic

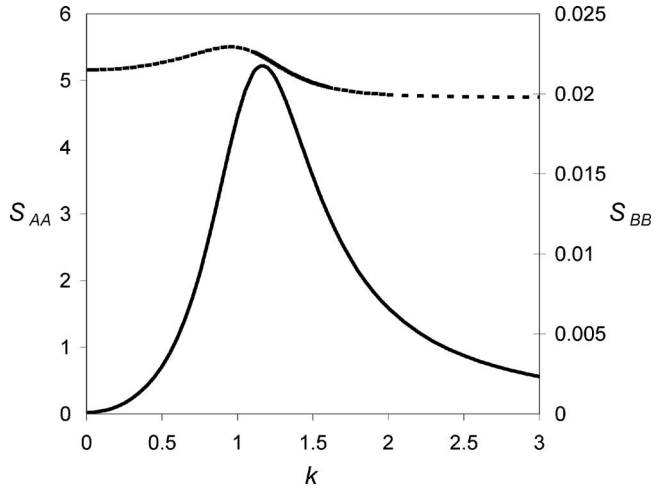

FIG. 2. Structure factor elements, s_{AA} (solid curve) and s_{BB} (dashed curve), calculated for $f=0.01$, $\chi=1$, $V_0=V_D=0$, $\mu_0=1$, and $\mu_D=\mu_F=0$.

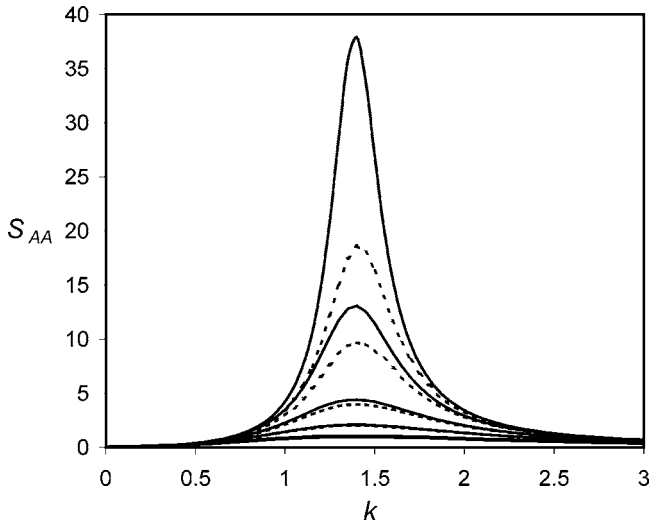

FIG. 3. Effects of cross-linking on the A-A scattering intensity, calculated for $f=0.01$, $\chi=1$. Solid and dashed curves correspond to $\mu_{AA}=\mu_{BB}=\mu_{AB}=0,1,1.5,1.8,1.9$ and $\mu_{AA}=0,1,1.5,1.8,1.9$, $\mu_{BB}=\mu_{AB}=0$, respectively.

coefficients of the free energy to give a matrix in terms of the partial monomer densities, ρ_A and ρ_B, expressed in terms of the replica symmetric order parameters through $\rho=\rho_A+\rho_B$ and $m/2=\rho_A(1-f)-\rho_B f$. The resulting scattering matrix is

$$\mathbf{S}^{-1}=\frac{1}{\beta}\begin{bmatrix} s_{AA} & s_{BA} \\ S_{AB} & s_{BB} \end{bmatrix}, \tag{19}$$

where

$$s_{AA}=\frac{1}{2}\left(\frac{a^2k^2}{2}+v_0(k)+4v_D(k)(1-f)+4\left(v_F(k)+\frac{1}{\sigma^2}\right)(1-f)^2\right),$$

$$s_{BB}=\frac{1}{2}\left(\frac{a^2k^2}{2}+v_0(k)-4v_D(k)f+4\left(v_F(k)+\frac{1}{\sigma^2}\right)f^2\right),$$

$$s_{AB}=s_{BA}=\frac{1}{2}\left(\frac{a^2k^2}{2}+v_0(k)+2v_D(k)(1-2f)-4\left(v_F(k)+\frac{1}{\sigma^2}\right)f(1-f)\right). \tag{20}$$

Figure 2 presents a typical plot of the structure factor for a cross-linked network consisting of a small fraction ($\sim 1\%-10\%$) of $\boldsymbol{B}$ monomers. The plot of s_{AA} exhibits a narrow peak corresponding to a typical scattering length, while the peak exhibited by the $\boldsymbol{B}$ monomers is broad and nearly indistinguishable. Although fluctuations in the concentration of the $\boldsymbol{B}$ monomers exist, due to the low fraction of $\boldsymbol{B}$ they remain relatively small.

Divergence of the scattering intensity indicates the emergence of an ordered phase [8]. The different elements of the structure factor all diverge at the same point [24], called the spinodal. For a copolymer system, $S(k)$ diverges when the fluctuations in the concentrations of the different monomers become exceedingly high and the disordered phase becomes unstable, indicating the onset microphase separation of the different monomers. In addition, the increase in scattering intensity with increased cross-linking in homopolymer gels has been attributed to cross-link density inhomogeneities, resulting in regions with high degrees of cross-linking separated by regions with a lower density of cross-links [29]. In our study of a cross-linked binary system, we find that several factors can lead to instability of the disordered phase, even for small fractions of $\boldsymbol{B}$. First, in Fig. 3 we see that increasing the degree of cross-linking sufficiently can *eventually* drive the network towards order, or microphase segregation of the different monomers, manifested in a diverging intensity peak of all elements of the structure factor. Comparison of the solid curves ($\mu_{AA}>0, \mu_{BB}=\mu_{AB}=0$) with the dashed curves ($\mu_{AA}=\mu_{BB}=\mu_{AB}>0$) reveals that cross-linking of only the backbone monomers (type A) can drive the system towards the inhomogeneous ordered phase at lower degrees of cross-linking. Clearly, in the former case the difference in functionality as well as interactions between the different monomers provides a greater drive for microphase segregation. Second, as is already well established both experimentally and theoretically, we see in Fig. 4 that increasing distinct interactions between the different monomers leads to microphase segregation which occurs at a particular wavelength for a given copolymer composition. Unlike the effect of increasing degrees of cross-linking, increasing the competitive interactions shifts the peak to smaller and smaller wavelengths or larger and larger domain sizes, while for strong mixing interactions, the peak is smeared since these conditions favor disorder. Comparison of Fig. 4 with Fig. 3 reveals that interactions play a more significant role in driving the system towards the ordered phase than do increasing degrees of cross-linking, as is apparent by the minor difference between two extreme cases of cross-linking.

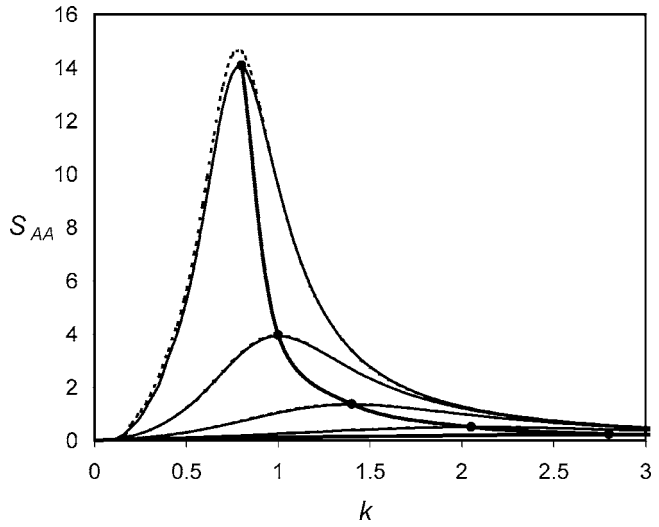

FIG. 4. Effects of competing monomer-monomer interactions on the *A*-*A* scattering intensity, calculated for $f=0.01$, $\chi=-10$, $-2,1,1.6$. Solid and dashed curves correspond to $\mu_{AA}=\mu_{BB}=\mu_{AB}=1$ and $\mu_{AA}=1$, $\mu_{BB}=\mu_{AB}=0$, respectively. —●— represents the relationship between peak wavelength and peak intensity.

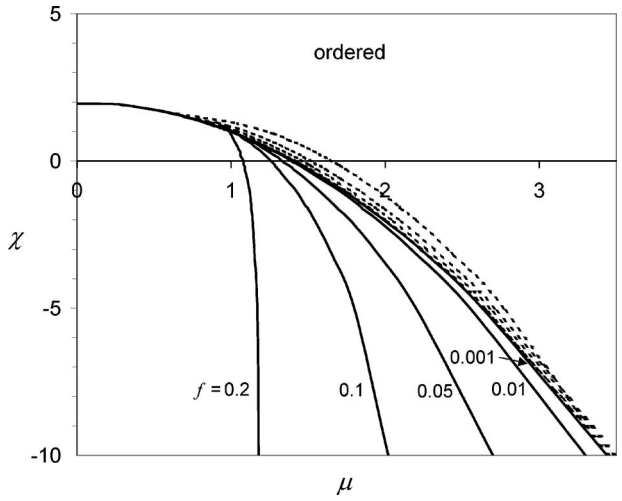

FIG. 5. Spinodal curve as a function of cross-linking and Flory interactions for various values of f. The spinodal presents the transition from a disordered (below the curve) to an ordered (above the curve) phase. Solid and dashed curves correspond to $\mu_{AA}>0$, $\mu_{BB}=\mu_{AB}=0$ and $\mu_{AA}=\mu_{BB}=\mu_{AB}>0$, respectively.

The spinodal for various values of f as a function of μ and χ is plotted in Fig. 5. Increasing the degree of cross-linking or the segregating interactions will drive the system towards order, though the homogeneous phase spans a larger range of these parameters for smaller values of f. As has been observed by Gallot [30], for a given composition of the copolymer, the structure can be changed with a preferential solvent. However, it appears that for sufficiently weak degrees of cross-linking ($\mu<1$) the spinodal, which is a weak function of μ is reached at a particular value of χ irrespective of the fraction of ***A*** monomers (the dashed curves in Fig. 5 reveal that the fraction of "imprinting" monomers has a small effect on the spinodal for the case of cross-linking of only the majority backbone monomers).

B. Ordered phase

Formation of ordered mesopores can be achieved through controlled phase segregation of cross-linked copolymers followed by selective removal of one of the components [31]. We consider the microphase segregated regime in the compact globular state. This state is characterized by a large number of chain conformations, for which density fluctuations can be neglected, which implies that terms in energy expression linear in $m(k)$ in Eq. (17) can be neglected. Indeed, a comprehensive study of the frozen behavior of physically cross-linked random heteropolymers carried out by Gutman and Shakhnovich [19,32] using a replica symmetry breaking scheme [33] reveals that highly nonsymmetric compositions ($f<0.1$) are found in the random goluble state even for relatively strong Flory interactions.

We consider the spatially homogeneous solution for non-excluded volume polymer, $V_0=0$, obtained from the single-replica Hamiltonian. In the compact state, we assume that the parameters characterizing the state of preparation dominate, i.e., average monomer density. In this case, the replica symmetric form of Eq. (17) reduces to

$$F[\rho,m]=\frac{1}{2}\sum_k[\rho(k)v_0(k)\rho(-k)+m(k)v_F(k)m(-k)]+\tilde{\varphi}(k=0)-\sum_{k\neq 0}\frac{\tilde{\varphi}(k)\tilde{\varphi}(-k)}{a^2k^2}-\frac{\sigma^4}{4}\sum_{k,k'\neq 0}\frac{\varphi_m(k)\varphi_m(-k)\varphi_m(k')\tilde{\varphi}_m(-k')}{a^2(k^2+k'^2)}-\sum_k[\varphi_\rho(k)\rho(-k)+\varphi_m(k)m(-k)]. \quad (21)$$

Differentiation with respect to $\rho(k)$ and $m(k)$ results in $\varphi_\rho(k)=\rho(k)v_0(k)$ and $\varphi_m(k)=m(k)v_F(k)$, respectively. Thus, the ground state solution of Eq. (21) is

$$\rho(k\neq 0)=-\frac{2\rho(k)v_0(k)}{a^2k^2}+\frac{\sigma^2}{a^2k^2}\sum_{k'\neq 0}m(k')v_F(k')m(k-k')v_F(k-k'), \quad (22)$$

$$m(k\neq 0) = -\sigma^2 m(-k)v_F(-k) - \sigma^2\sum_{k'}\frac{\rho(k')v_0(k')m(k'-k)v_F(k'-k)}{a^2k'^2} - \sigma^2\sum_{k'}\frac{\rho(k')v_0(k')m(-k'-k)v_F(-k'-k)}{a^2k'^2}$$
$$-\sigma^4\sum_{k',k''}\frac{m(k'-k)v_F(k'-k)m(k'')v_F(k'')m(-k'-k'')v_F(-k'-k'')}{a^2k'^2}$$
$$-\sigma^4\sum_{k'}\frac{m(-k)v_F(-k)m(k')v_F(k')m(-k')v_F(-k')}{a^2(k^2+k'^2)}. \quad (23)$$

Equations (22) and (23) are solved self-consistently for $m(k)$ and $\rho(k)$. Typical plots of the microphase order parameter for several values of the Flory interaction parameter are shown in Fig. 6. For the case of cross-links that are independent of monomer type (solid curves), at zero interactions but finite degree of cross-linking there is no phase separation. As expected, it is seen that stronger segregating interactions lead to finer decomposition, which would give rise to more distinct cavities once the B imprinting monomers are removed. However, when only the majority monomers are allowed to cross-link (dashed curves), then microphase segregation is observed even for an athermal system ($\chi=0$), with a different periodicity, that is again intensified with increasing segregating interactions. That is, the type of cross-linking affects the final morphology of the gel while interactions enhance the degree of segregation.

Changes in the amplitude of the relative density of the majority phase and microphase order parameters as a function of interaction strengths are plotted in Fig. 7(a) and as a function of cross-linking potential (μ_0) in Fig. 7(b). Interestingly, a monotonic increase in the amplitudes of ρ and m in Fig. 7(a) is observed, indicating a linear dependency of the tendency toward microphase separation on the segregating interactions between the different monomers. It is also seen that increasing the degree of cross-linking leads to an increase in local density fluctuations while the order parameter remains unchanged. The latter is expected since the cross-linking potential was assumed to be independent of monomer type. In fact, when μ_{AA} is varied for a given interaction strength fluctuations in the order parameter are seen to increase with the degree of cross-linking (results not shown).

From the results presented in Figs. 3–7, it can be concluded that control over the degree of cross-linking and the competing monomer interactions can be used together to produce porous structures of a specified size beyond the spinodal. That is, a particular domain size is chosen through

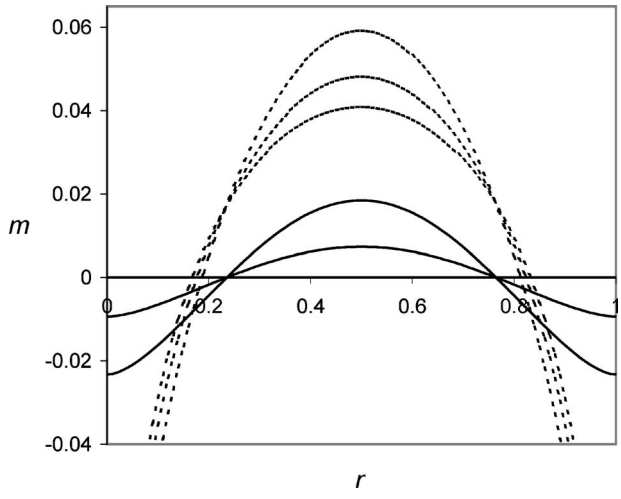

FIG. 6. Periodicity of the microphase order parameter in the ordered phase for $\mu_{AA}=\mu_{BB}=\mu_{AB}=0.75$ (solid) and $\mu_{AA}=0.75$, $\mu_{BB}=\mu_{AB}=0$ (dashed) for $f=0.01$ and different values of the Flory interaction parameter. Curves showing increasing microphase separation are for $\chi=0$, $\chi=2$, and $\chi=5$.

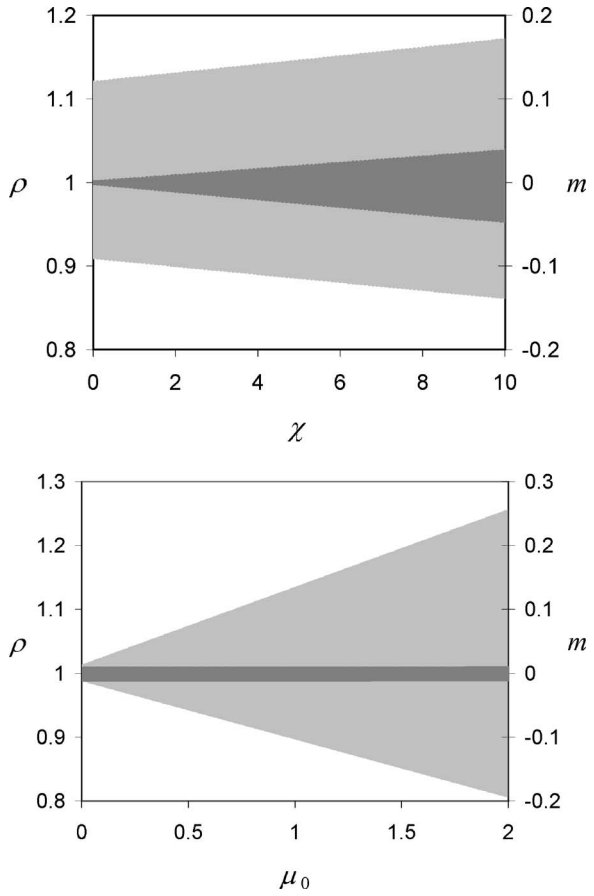

FIG. 7. Changes in positive and negative amplitudes of the relative density of the majority phase (light gray) and microphase (dark gray) order parameters for $f=0.01$ as a function of (a) Flory interactions for $\mu_0=1$ and (b) cross-linking potential, μ_0, for $\chi=2$.

selection of an appropriate solvent typified by certain χ, while high degrees of cross-linking can be used to quench the system at this particular domain size.

IV. CONCLUSIONS

We presented a mean-field model of a physically cross-linked random copolymer consisting of a small fraction of monomers acting as imprinting agents, which are in principle removable following gel formation. We examined the effects of cross-linking and interactions on phase segregation between the two types of monomers. The disordered phase, characterized by a relatively homogeneous dispersion of the minority group, is favored by small or negative χ (tending towards mixing interactions) and lower cross-linking densities. Such conditions are advantageous, e.g., for molecular imprinting applications since successful imprinting requires evenly distributed sites. However, in practice, a relatively rigid network is required in order to preserve the characteristics of the imprinting agents, which is in general achieved using high degrees of crosslinking. Therefore, an optimum between the degree of cross-linking and tendency towards aggregation must be found. On the other hand, conditions favoring microphase-segregated configurations are advantageous for controlling the porous structure of the gel, where the minority monomers present a removable group. In this case, cavity size can be controlled through cross-linking density, monomer interactions, and type of solvent.

ACKNOWLEDGMENTS

This research was supported, in part, by the Israel Science Foundation and the P. and E. Nathan Research Fund. The author acknowledges being a Koebner-Klein Scholar.

APPENDIX

The following details the calculation of the effective entropy appearing in the partition function of Eq. (14). The squared term in Eq. (16) can be expanded into symmetric and nonsymmetric terms in the replica index, α, as follows:

$$\frac{\sigma^2}{2}\left(\sum_\alpha \varphi_m^\alpha\right)^2\psi^\alpha = \frac{\sigma^2}{2}\sum_\alpha \varphi_m^{\alpha^2}\psi^\alpha + \frac{\sigma^2}{2}\sum_{\alpha\neq\beta}\varphi_m^\alpha\varphi_m^\alpha\psi^\alpha. \quad \text{(A1)}$$

Letting $\tilde{\varphi}^\alpha = \varphi_\rho^\alpha - (\sigma^2/2)\varphi_m^{\alpha^2}$ and rewriting Eq. (17) using $\tilde{\varphi}^\alpha$ and Eq. (A1) gives

$$\left(-a^2\sum_\alpha \nabla^{\alpha^2} + \sum_\alpha \tilde{\varphi}^\alpha(r^\alpha) - \frac{\sigma^2}{2}\sum_{\alpha\neq\beta}\varphi_m^\alpha(r^\alpha)\varphi_m^\alpha(r^\alpha)\right)\psi^\alpha = \sum_\alpha \lambda\psi^\alpha. \quad \text{(A2)}$$

To proceed, Eq. (A2) is transformed to Fourier space, where $k \sim a\ell^{1/2}/6^{1/2}$ and ℓ is the average block length of the polymer. Perturbation expansion of λ for small ρ and m gives [26]

$$\lambda N|_{k\neq 0} = \sum_\alpha \tilde{\varphi}^\alpha(k=0) - \sum_\alpha\sum_{k\neq 0}\frac{\tilde{\varphi}^\alpha(k)\tilde{\varphi}^\alpha(-k)}{a^2k^2} - \frac{\sigma^4}{4}\sum_{\alpha\neq\beta}\sum_{k,k'\neq 0}\frac{\varphi_m^\alpha(k)\varphi_m^\alpha(-k)\varphi_m^\alpha(k')\varphi_m^\alpha(-k')}{a^2(k_1^2+k_2^2)}. \quad \text{(A3)}$$

The entropy is calculated by expressing Z^p, and thus φ_ρ^α and φ_m^α, in terms of m_α and ρ_α using the definition $\ln Z^p = -\lambda N$. The solution of Eq. (15) yields

$$\rho^\alpha(k=0) = 1,$$

$$\rho^\alpha(k\neq 0) = -\frac{2\varphi_\rho^\alpha(-k)}{a^2k^2} + \frac{\sigma^2}{a^2k^2}\sum_{k'\neq 0}\varphi_m^\alpha(k')\varphi_m^\alpha(k-k'), \quad \text{(A4)}$$

$$m^\alpha(k\neq 0) = -\sigma^2\varphi_m^\alpha(-k) - \sigma^2\sum_{k'}\frac{\varphi_\rho^\alpha(k')\varphi_m^\alpha(k'-k)+\varphi_\rho^\alpha(k)\varphi_m^\alpha(-k'-k)}{a^2k'^2} - \sigma^4\sum_{k',k''}\frac{\varphi_m^\alpha(k'-k)\varphi_m^\alpha(k'')\varphi_m^\alpha(-k'-k'')}{a^2k'^2} - \sigma^4\sum_{\beta\neq\alpha}\sum_{k'}\frac{\varphi_m^\alpha(-k)\varphi_{m,b}^\beta(k')\varphi_m^\beta(-k')}{a^2(k^2+k'^2)}. \quad \text{(A5)}$$

These expressions can now be used to solve for the entropy appearing in Eq. (14).

[1] V. Sfika and C. Tsitsilianis, Macromolecules **36**, 4983 (2003).
[2] H. Y. Wang, T. Kobayashi, and N. Fujii, Langmuir **12**, 4580 (1996).
[3] M. Yoshikawa, J.-i. Izumi, T. Kitao, and S. Sakamoto, Macromolecules **29**, 8197 (1996).
[4] G. Wulff and A. Sarhan, Angew. Chem., Int. Ed. Engl. **11**, 341 (1972).
[5] R. Arshady and K. Mosbach, Makromol. Chem. **182**, 687 (1981).
[6] M. Ramamoorthy and M. Ulbricht, J. Membr. Sci. **217**, 207 (2003).
[7] R. Malaisamy and M. Ulbricht, Sep. Purif. Methods **39**, 211 (2004).
[8] P. G. de Gennes, *Scaling Concepts in Polymer Physics* (Cornell University Press, Ithaca, 1979).
[9] R. C. Ball, M. Doi, S. F. Edwards, and M. Warner, Polymer **22**, 1010 (1981).
[10] P. G. Higgs and R. C. Ball, Europhys. Lett. **8**, 357 (1989).
[11] J. Huh, S. H. Kim, and W. H. Jo, Macromolecular Research **10**, 18 (2002).

[12] A. L. R. Bug, M. E. Cates, S. A. Safran, and T. A. Witten, J. Chem. Phys. **87**, 1824 (1987).
[13] L. Leibler, M. Rubinstein, and R. H. Colby, J. Phys. II **3**, 1581 (1993).
[14] L. Huang, X. H. He, L. S. Huang, and H. J. Liang, Polymer **44**, 1967 (2003).
[15] P. G. Khalatur, A. R. Khokhlov, J. N. Kovalenko, and D. A. Mologin, J. Chem. Phys. **110**, 6039 (1999).
[16] N. Urakami and M. Takasu, J. Phys. Soc. Jpn. **65**, 2694 (1996).
[17] A. R. C. Baljonhaakman and T. A. Witten, Macromolecules **25**, 2969 (1992).
[18] M. Rubinstein and A. N. Semenov, Macromolecules **34**, 1058 (2001).
[19] L. Gutman and E. Shakhnovich, J. Chem. Phys. **107**, 1247 (1997).
[20] R. T. Deam and S. F. Edwards, Philos. Trans. R. Soc. London, Ser. A **280**, 317 (1976).
[21] R. C. Ball and S. F. Edwards, Macromolecules **13**, 748 (1980).
[22] R. P. H. Feynman, *Quantum Mechanics and Path Integrals* (McGraw-Hill, New York, 1965).
[23] K. H. H. Fischer and A. John, *Spin Glasses* (Cambridge University Press, Cambridge, 1991).
[24] L. Leibler, Macromolecules **13**, 1602 (1980).
[25] P. Goldbart and N. Goldenfeld, Phys. Rev. A **39**, 1412 (1989).
[26] E. I. Shakhnovich and A. M. Gutin, J. Phys. (France) **50**, 1843 (1989).
[27] T. Garel, D. A. Huse, S. Leibler, and H. Orland, Europhys. Lett. **8**, 9 (1989).
[28] A. K. Chakraborty, J. Chem. Phys. **111**, 5232 (1999).
[29] J. Bastide and J. S. Candau *The Physical Properties of Polymer Gels* (Wiley, New York, 1996).
[30] B. R. M. Gallot, Adv. Polym. Sci. **29**, 85 (1978).
[31] K. Nakanishi, J. Sol-Gel Sci. Technol. **19**, 65 (2000).
[32] L. Gutman and E. Shakhnovich, J. Chem. Phys. **114**, 10968 (2001).
[33] M. Mezard and G. Parisi, J. Phys. I **1**, 809 (1991).